Water Bath Calorimetry (031621): Report

M. Nansteel (April, 2021)

Summary

A single water bath calorimetric measurement of plasma energy release was observed on March 16, 2021 at BLP, Cranbury. This test featured a new 10 inch diameter dual electrode plasma cell which operated at temperatures exceeding 700°C in the power phase. The high temperature resulted, in part, from the insulating effects of a three-piece C/Mo/W liner deployed inside the cell. The energy released by the plasma was determined from sensible heating of the bath as well as a measurement of the mass of water boiled off and various other energy effects including electrical energy input and thermal losses from the bath. The plasma energy release was calculated using a rigorous statement of energy conservation. The present document provides a detailed description of the test apparatus, conditions and procedures used in the tests, the energy balance formulas applied in the calorimetric evaluation, and analysis of the test data to obtain the plasma energy release.

The calorimetric test encompassed two phases. In the preheating phase the cell temperature was increased to greater than 400°C and the water bath temperature to very near 100°C. This was followed by the power phase in which power and energy flows were carefully measured in order to determine the plasma energy release. The mass of bath water lost by boiling during the preheat phase was determined from a control experiment in which conditions closely matched conditions during the preheat phase. This is a key feature of the present calorimetric method.

During the power phase, very vigorous boiling was observed on the outer surface of the cell suggesting a high rate of heat rejection to the bath. Over the ~62 s power phase the average cell temperature was 583°C and the maximum temperature was 716°C. Plasma performance in the test is summarized by

$$E_{\text{Elect}} = 4008 \text{ kJ}, \qquad E_{\text{Plasma}} = 10{,}481 \text{ kJ}$$

and

$$\text{Gain} = \frac{E_{\text{Plasma}} + E_{\text{Elect}}}{E_{\text{Elect}}} = 3.62$$

These results indicate that the plasma energy release is 262% of the electrical energy required to maintain the plasma.

The average plasma power during the 61.9 s duration power phase was

$$P_{\text{Plasma}} = 169 \text{ kW}$$

However, if most of the energy was released later in the power phase, after the electrode power stabilized, then a more accurate power estimate, based on a 50 second release period, is

$$P_{\text{Plasma}} = 210 \text{ kW (based on 50 s energy release period)}$$

If the electrode power remains at the average level of ~65 kW during the time that this increased plasma power release is occurring, then the local power gain is about 4.2.

In the measurement of plasma energy, the largest contribution to the energy balance is the energy due to vaporization of the mass δm_w of bath water. The measurement of δm_w was subject to about ±0.1 kg uncertainty which carried through the energy balance calculation, but this uncertainty corresponded to only about a ±2% uncertainty in the plasma energy release.

Critical data collected in the two calorimetric tests conducted on 12/04/20 are compared with the data from the present test in Table S1. This table features the gallium working fluid mass and time duration of the power phase in each test as well as the average cell temperature, the approximate glow discharge voltage, current and power, water boil-off, and performance data such as plasma energy, power and gain. In the present test conducted with the new, larger dual electrode cell at an average temperature of 583°C the performance clearly exceeds that achieved in the prior tests using a single electrode in a smaller cell, running at lower temperature. In particular, the average plasma power has increased by about 82% relative to the best performance measured in December, 2020.

Table S1. Summary of results in calorimetric tests: 03/16/21 and 12/04/20

Test date		m_{Ga} [kg]	Δt [s]	T_{Cell} [°C]	V_{GD} [V]	I_{GD} [A]	P_{GD} [W]	δm_w [kg]	E_{Plasma} [kJ]	E_{Elect} [kJ]	Gain	P_{Plasma} [kW]
03/16/21		8.8	61.9	583	300	0.53	159	6.5	10,481	4008	3.62	169
12/04/20	Run 1	6	167	458	0	0	0	7.1	9313	6951	2.34	55.8
	Run 2	6	200	425	310	0.38	118	11.5	18,592	7800	3.38	93.0

Background

A single calorimetric test was observed on March 16, 2021 at BLP, Cranbury. The test was conducted in order to document the plasma energy release from a newly designed, larger Cr-Mo steel reactor cell. The plasma cell was operated in a water bath, as usual, in order to capture and measure as much of the energy release as possible. A new dual electrode cell design was used with higher operating temperature than the tests in December, 2020 to further increase plasma output. Higher temperature was achieved, in part, by a three-piece carbon/molybdenum/tungsten liner which partially insulated the high temperature liquid gallium from the cooler cell wall. In the present test this results in cell temperature exceeding 700°C at the end of the power phase. A separate control experiment was used to estimate the water boil-off in the preheat phase, as in the December tests.

This document includes description of the test apparatus and conditions, documentation of the energy conservation formula applied in the calorimetric measurement, and analysis of the test data to obtain the plasma energy release.

Plasma cell description

The new plasma cell is comprised of a vertical chrome-molybdenum steel tube, now with 10 inch OD and 0.05 inch wall thickness. A supplemental cylindrical chamber, made from a 4 inch OD chrome-molybdenum tube, also with 0.05 inch wall, is welded to the main chamber as shown in Fig. 1. The cell is partially filled with about 8.8 kg of liquid gallium which is recirculated through two stainless U-tubes by a pair of electromagnetic (EM) pumps, resulting in two vertical jets of liquid metal as sketched in Fig. 1. The jets impinge on separate tungsten electrodes and the high current plasma is formed by a low DC voltage which is maintained between the gallium jets and the electrodes. The cell wall is shielded from the plasma by a three-piece liner consisting of concentric layers of carbon, molybdenum and hexagonal plates of tungsten, ranging in thickness from 3 to 4 mm each, and radially spaced by about the same distance. The spaces between the layers trap stagnant gallium, hence reducing convection transfer to the cooler cell wall. This feature partially insulates the gallium from the wall and thereby increases cell temperature. The internal temperature of the cell is measured by a K-type ungrounded, quartz sheathed thermocouple probe (not shown in Fig. 1) immersed in the liquid gallium.

Either pure hydrogen flows through the cell and is continuously evacuated, or hydrogen is mixed with trace oxygen and reacted outside the cell and the bath in the glow discharge cell before flowing through the cell, as shown in Fig. 1. A vertical tube fitted with an electrode is attached to the upper flange of the cell so that a glow discharge can be maintained there. Dissociation of the hydrogen gas flow and formation of trace H_2O, resulting from the glow discharge process, is thought to be a key feature of the plasma reaction.

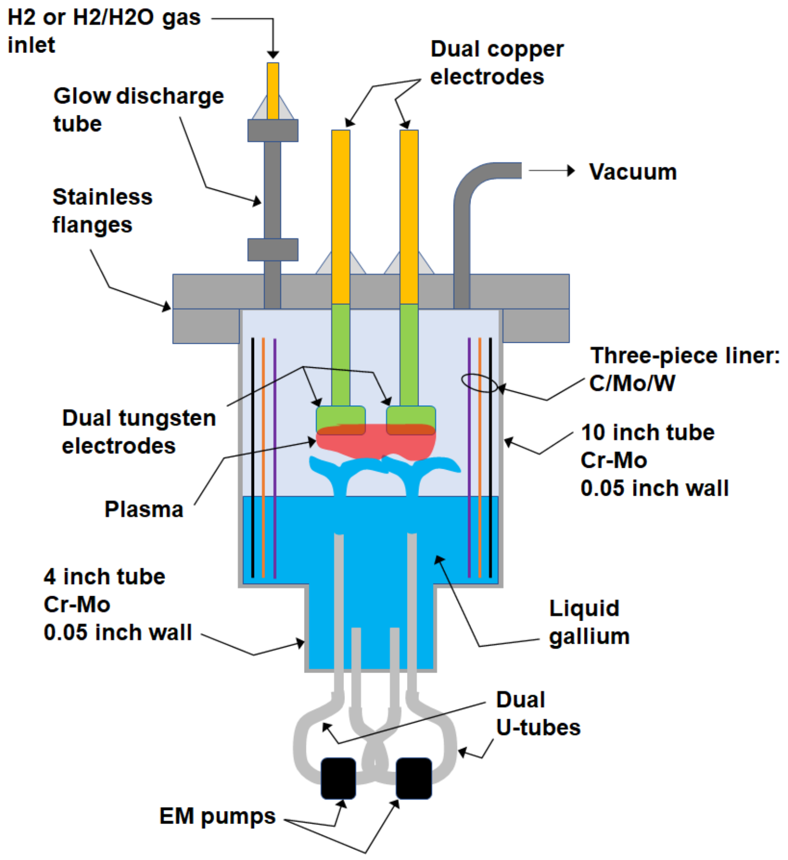

Figure 1. Schematic diagram of plasma cell with dual electrodes and three-piece liner

Calorimetric measurement procedure

The water bath calorimetric measurement of plasma energy is achieved in a two-phase process which was described in connection with the December, 2020 tests. First, a preheating phase with mostly fixed electrode power input is used to heat the cell to near 400°C and the bath water up to near boiling temperature. During the subsequent power phase the electrode power is increased and a glow discharge is maintained in the glow discharge cell. During this phase the power inputs, the bath temperature rise, and bath vaporization losses are carefully measured so that an accurate calorimetric measurement of the plasma heat release is possible. The water boil-off during the preheat phase is estimated from the boil-off measured during a control experiment in which conditions are very similar to the preheat phase. The system and auxiliary tanks used for measuring the change in water mass and water boil-off were similar to those used in December, 2020, however, the system tank incorporated only one water jet pump in the present test.

Preheat phase

During the preheating phase liquid gallium circulation is maintained by the two EM pumps and the plasma is maintained in the cell with a modest electrode power level near 35 kW (total). A 4000 sccm flow of pure hydrogen is delivered to the cell and no glow discharge is used during the preheat phase. The single water jet pump is operated continuously until the bath temperature reaches approximately 90°C. Due to the electrode power input and modest plasma energy release during the early stages of the preheat phase, the bath water is heated by both convection and subcooled boiling at the cell surface. And because the bath water is well below the water saturation temperature, most of the generated vapor condenses before escaping from the bath surface. Nevertheless, vapor is continually lost from the bath free surface, and at an increasing rate as the bath temperature increases. The gallium temperature in the cell is monitored by a single thermocouple probe and the bath water temperature is monitored, similarly, by a single thermocouple probe immersed in the bath. When the bath temperature reaches approximately 90°C the water jet pump shuts down owing to self-protection circuitry in the pump. At this time vigorous nucleate boiling occurs at the cell surface. At the end of the approximately 24 minute preheat phase, the bath temperature has nearly reached 100°C and the cell temperature is near 400°C. At this time the preheat phase of the test ends and the power phase begins.

Power phase

During the power phase the plasma electrode current is stepped up relative to the preheat phase to about 1.5 kA for each electrode. The hydrogen flow is maintained at 4000 sccm and, in addition, 3 sccm of oxygen is mixed with the hydrogen outside the cell and the bath and flowed through the discharge cell into the cell. The glow discharge is maintained with about a 300 volt differential in the glow discharge tube. The electrode voltage and current are continuously recorded during the power phase with a sampling frequency of 5 kHz (5 samples every millisecond or one sample every 200 μs). The voltage and current supplied to the two EM pumps and the glow discharge during the power phase are also noted, however, these parameters are known less precisely because the corresponding data are not recorded by the data acquisition system (DAS). Also, the cell/gallium and bath temperatures are logged to computer memory once every second. During this period of strong cell heat release the bath water is nearly at 100°C so vigorous nucleate boiling occurs at the cell surface and most of the vapor generated escapes from the bath free surface. The power phase of the test run is terminated after about 60 s of operation. At this time electrode power to the cell ceases and power to the EM pumps and the glow discharge is removed.

Post-power phase

After the power phase is complete, the water in the bath is pumped from the system tank back to the auxiliary tank without delay. Only the same small volume of water which was originally in the system tank is allowed to remain. The mass of water pumped into the auxiliary tank is weighed by the same mass scale used to measure the initial mass. This water mass is compared to the mass initially pumped into the system tank and the difference is the mass of water lost as vapor during both the preheat and power phases of the test.

Control experiment

The vapor loss during the preheating phase is determined in a separate control experiment in which conditions are maintained nominally the same as those prevailing during the preheating phase. That is, the bath water temperature, electrode power and EM pump power are nominally the same as in the preheating phase. In this way the amount of vapor loss during the control experiment is very nearly the same as in the preheating phase. The mass of this vapor loss is easily determined at the conclusion of the control experiment by transferring the water to the auxiliary tank as described above.

Electrode and EM pump power supplies, and instrumentation

Electrode power was supplied by a pair of LabView-controlled switch mode rectifiers (American CRS Q500 IP32). Electrode voltage was monitored using differential probes (PicoTech TA041, ±70 V) and current was monitored by DC Hall effect sensors (GMW CPCO-4000-77-BP10, ±4kA). Electrode voltage and current were sampled by a high-resolution oscilloscope (PicoScope 5000 Series) at 5 kHz sampling rate. The two EM pumps were powered by a single programmable DC power supply (Matsusada Precision REK10-1200) in current control mode. The resulting current and voltage supplied to the pumps was very stable and therefore these data were not saved by the DAS, but rather the mostly constant current and voltage were recorded manually. The glow discharge current and voltage were similarly monitored and manually recorded. The hydrogen (4000 sccm) and oxygen (0 or 3 sccm) flows were controlled by separate mass flow controllers (MKS 1179A53CR1BVS for H_2 and MKS M100B12R1BB for O_2). The single bath water jet pump was a Little Giant 5-MSP (1200 gph at 1 foot head, 125 W). The cell internal temperature was monitored by a K-type (ungrounded), quartz sheathed thermocouple probe which extended about one cm into the gallium pool. Bath temperature was measured by a single thermocouple probe which was immersed in the bath several inches below the water surface, near the bath wall. The single probe for measuring bath temperature is thought to be sufficient since bath water temperature is spatially uniform (near 100°C) and varies temporally by only a fraction of a degree during the power phase. Cell temperature and bath temperature data were sampled at one second intervals and saved by the data acquisition system.

Energy conservation

The basis for applying energy conservation is a deformable, open thermodynamic system consisting of the water in the bath as well as the cell and related immersed components, e.g. the EM pumps, jet pump, interconnecting power cables, etc. The energy conservation equation is derived in the report on the calorimetry tests conducted on November 10, 2020. After simplification, energy conservation applied to the power phase takes the form

$$E_{\text{Plasma}} = \left\{ \begin{array}{l} m_{w1}(h_{w2} - h_{w1}) - \delta m_w \left(h_{vap2} + (h_{v,lost} - h_{v2}) \right) + \sum_j m_j (h_{j2} - h_{j1}) \\ -E_{\text{Elect}} - E_{\text{EMP}} - E_{\text{GD}} - [E_{\text{WJ}} - Q_{\text{Loss}}] - \sum\limits_{\text{H2,H2O}} m(h_i - h_e) \end{array} \right\}$$

in which the times t_1 and t_2 correspond to the start and end of the power phase, E and h denote energy and specific enthalpy, m_{w1} and δm_w are the mass of water in the bath at time t_1 and the change in mass during the time interval $t_1 < t < t_2$, and h_{vap2} and h_{v2} are the enthalpy of vaporization and enthalpy of saturated vapor, each at the bath temperature at the end of the power phase (time t_2). The enthalpy $h_{v,lost}$ is the specific enthalpy of the vapor lost from the bath surface during the process. The final summation is the net enthalpy entering the bath due to the H_2/H_2O gas through-flow. The electrode, EM pump and glow discharge energy terms are the integrated power inputs during the power phase

$$E_{\text{Elect}} = \int_{t_1}^{t_2} P_{\text{Elect}}\,dt, \quad E_{\text{EMP}} = \int_{t_1}^{t_2} P_{\text{EMP}}\,dt, \quad E_{\text{GD}} = \int_{t_1}^{t_2} P_{\text{GD}}\,dt$$

and the m_j and h_j denote the masses and specific enthalpies of the various components in the bath such as the cell parts, the gallium working fluid, the EM pumps, the water jet pump, etc. The corresponding thermal mass data are tabulated in Table 1.

Table 1. Component masses, specific heats and thermal masses

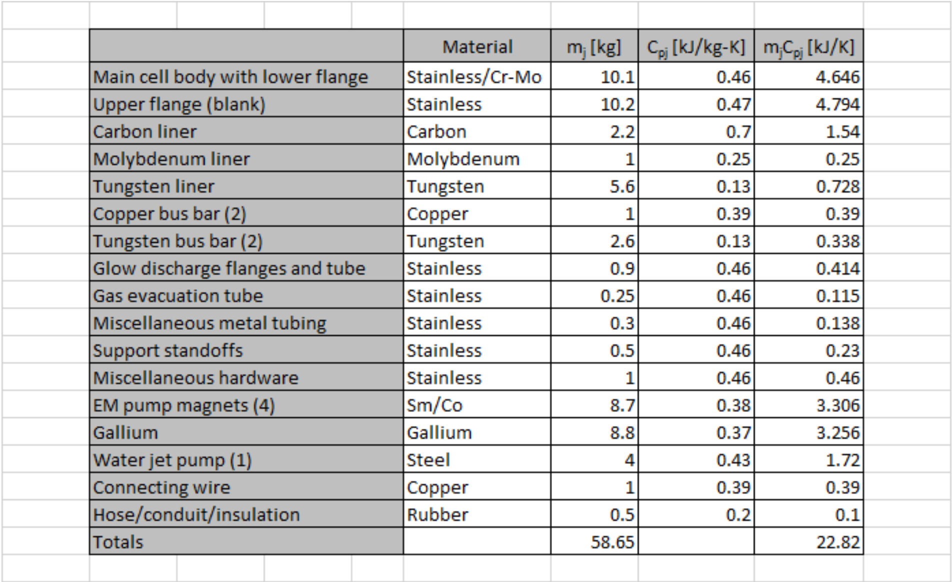

	Material	m_j [kg]	C_{pj} [kJ/kg-K]	m_jC_{pj} [kJ/K]
Main cell body with lower flange	Stainless/Cr-Mo	10.1	0.46	4.646
Upper flange (blank)	Stainless	10.2	0.47	4.794
Carbon liner	Carbon	2.2	0.7	1.54
Molybdenum liner	Molybdenum	1	0.25	0.25
Tungsten liner	Tungsten	5.6	0.13	0.728
Copper bus bar (2)	Copper	1	0.39	0.39
Tungsten bus bar (2)	Tungsten	2.6	0.13	0.338
Glow discharge flanges and tube	Stainless	0.9	0.46	0.414
Gas evacuation tube	Stainless	0.25	0.46	0.115
Miscellaneous metal tubing	Stainless	0.3	0.46	0.138
Support standoffs	Stainless	0.5	0.46	0.23
Miscellaneous hardware	Stainless	1	0.46	0.46
EM pump magnets (4)	Sm/Co	8.7	0.38	3.306
Gallium	Gallium	8.8	0.37	3.256
Water jet pump (1)	Steel	4	0.43	1.72
Connecting wire	Copper	1	0.39	0.39
Hose/conduit/insulation	Rubber	0.5	0.2	0.1
Totals		58.65		22.82

The energy contribution due to the hydrogen and water vapor flow through the cell is shown in previous tests to be on the order of only 1 kJ, which is negligible compared to other energy terms in the balance, so it is ignored. Also, the term $E_{WJ} = 0$ since the water jet pump shuts down prior to the start of the power phase at time t_1. The term Q_{Loss} is the heat loss from the bath by heat convection and conduction to the lab, estimated from a measurement of bath temperature decay for bath temperatures between about 85 and 96°C. The rate of heat loss was found to be about 2.4 kW. This estimate is thought to have an uncertainty as large as ±50% for reasons discussed in the report on the tests conducted in December, 2020. Also, the difference $h_{v,lost} - h_{v2}$, which is the difference between the enthalpy of the vapor leaving the bath surface and the enthalpy of saturated vapor at the final bath temperature, is almost zero because the bath temperature during the power phase is nearly 100°C. In any case this difference is completely negligible compared with the enthalpy of vaporization h_{vap2}. With these simplifications the plasma energy release in the power phase reduces to

$$E_{Plasma} = m_{w1}(h_{w2} - h_{w1}) - \delta m_w h_{vap2} + \sum_j m_j(h_{j2} - h_{j1}) + Q_{Loss} - E_{Elect} - E_{EMP} - E_{GD} \quad (1)$$

where it is also noted that the change in bath water mass $\delta m_w < 0$, so vaporization corresponds to a positive contribution to E_{Plasma}.

Control experiment (031621)

A single control experiment was conducted to estimate the vapor loss during the preheat phase in the power run. The control experiment began with 197.4 kg of water added to the system tank. During the control the electrode and EM pump power were maintained at about 32 and 0.9 kW, respectively, and the pressure in the cell was about 7 Torr.

The cell/gallium and bath water temperature histories in the control experiment are plotted in Fig. 2. The beginning and end of the control experiment were correlated with the sudden temperature rise and fall of the cell corresponding, approximately, to the start and end of electrode power input. Using this procedure, the control experiment had a duration of about 1459 s. The cell temperature increased rapidly during the initial phase of the control due primarily to electrode power and probably some power release by the plasma. The gallium temperature increased to about 480°C and then gradually decayed to about 400°C at the end of the control. The bath water temperature increased mostly linearly, reaching about 97°C at the time of shut-down. The indicated bath water temperature exhibited a slow but temporary decay beginning at about 1200 s. Then, near ~1325 s the bath temperature rapidly increased again to a level consistent with the previous linear temperature rise, cf. Fig. 2. This effect is probably not a real variation of the bath temperature. Instead, it might be due to the bath thermocouple being temporarily withdrawn from the water, resulting in slow cooling in the hot air/vapor mixture just above the water surface. And, the rapid temperature recovery is consistent with the probe being re-immersed in the bath. During the later part of the control experiment, vigorous and mostly saturated nucleate boiling occurred at the cell surface. Water boil-off was found to be 6.8 kg by the differential weighing procedure described above. The temperatures and conditions during the control experiment are summarized in Table 2.

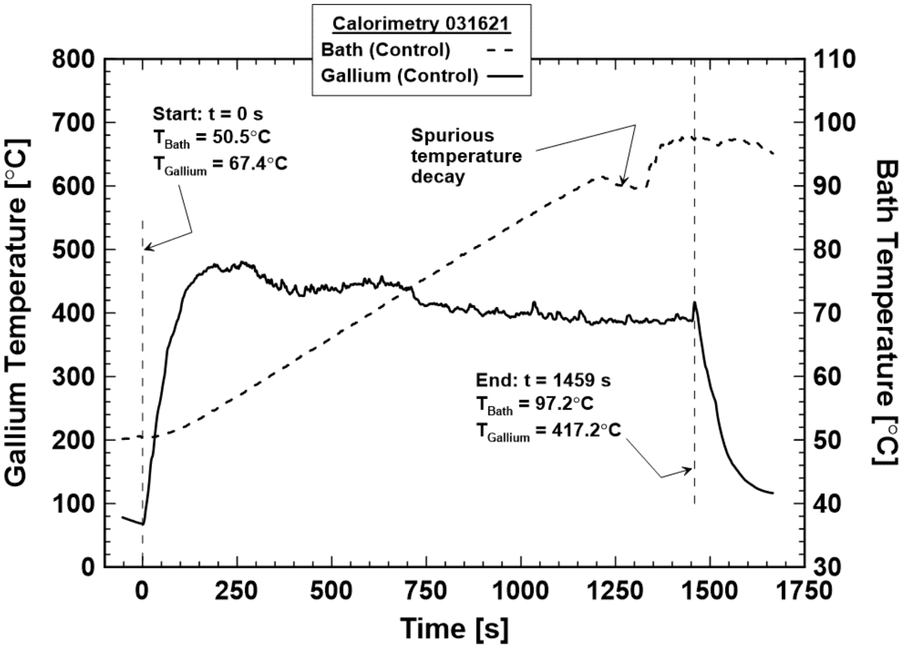

Figure 2. Cell and bath temperature histories in control experiment

Table 2. Control experiment summary

Start t = 0	T_{Ga} = 67.4°C; T_{Bath} = 50.5°C
Water mass	197.4 kg
Supplies 1 and 2	~0.75 kA; ~21 V; ~15.8 kW
EMP	710 A; 1.28 V; 909 W
Glow discharge	Off
Gas flow	4000 sccm H2
WJ pump	Running for T_{Bath} < 90°C
End t = 1459 s	T_{Ga} = 417.2°C; T_{Bath} = 97.2°C
Water mass	190.6 kg
Boil-off	6.8 kg

The cell and bath temperature behaviors plotted in Fig. 2, taken together, infer the rate of vapor loss from the bath at each time. Very high cell surface temperature or very high bath temperature do not necessarily indicate a high rate of vapor loss. Rather, it is high cell surface temperature in excess of the water saturation temperature coupled with bath temperature near saturation which results in rapid vapor bubble formation at the cell and low condensation during bubble rise in the bath liquid. These conditions, when present simultaneously, result in a high rate of vapor loss from the bath. For this reason the cell and bath temperature histories during the preheat phase of the calorimetric test will be compared with the corresponding histories during the control. If the temperature histories coincide for the preheat phase and the control, then it is reasonable to conclude that the water mass boil-off during the preheat and the control are the same.

Power run (031621)

Preheat phase

The preheat phase of the power run began with 197.4 kg of water in the system tank, the same mass as in the control experiment. Both the cell and bath water were near 50°C at the start of the preheat. Bath and cell temperature histories are plotted in Fig. 3 for the preheat phase of the power run and the control experiment such that t = 0 corresponds to application of electrode power (as indicated by the sharp rise in cell temperature) for both the control and preheat. This allows for direct comparison of the control and preheat. The end of the preheat phase is taken as the time when the cell temperature begins its sharp rise corresponding to the electrode power increase at the start of the power phase. This occurs at 1466 s, cf. Fig. 3.

The bath temperatures during the control and preheat phases are the same to within one or two degrees except between about 1050 and 1350 s. In this time period the same type of variations in indicated bath temperature occur for the preheat and control. These are not thought to be actual bath temperature variations but rather they are probably due to removal and re-immersion of the bath thermocouple probe as discussed above in relation to the control experiment. If this is the case, then the bath temperatures in the control and preheat are very similar throughout the duration of each. However, the cell/gallium temperatures in the control and preheat phase are less similar. In the early part of the preheat, for $t < 750$ s, the cell in the control is hotter than in the preheat by as much as 100°C. This leads to somewhat greater vaporization in the control relative to the preheat. This difference has the effect of lowering the estimated plasma energy release because it leads to under-estimation of the boil-off during the power phase. However, the effect is probably small because the bath temperature during this early period is less than about 70°C, suggesting that most of the vapor bubbles created at the cell surface re-condense before escaping the bath.

Later in the preheat phase ($t > 750$ s) the cell temperature exceeds the cell temperature in the control by as much as 60°C. This results in greater vaporization during the preheat than the control, which may result in over estimation of the plasma energy release because the boil-off during the power phase is then over-estimated. The effect of the cell temperature difference (preheat vs. control) during this later period may be more significant than for $t < 750$ s because the bath temperature is higher so that a greater fraction of the vapor bubbles generated at the cell surface rise to the bath surface and escape. The effect is not expected to substantially impact the plasma energy release estimate, however, it is recommended that in future calorimetric tests the cell electrode power during the preheat should be regulated, if possible, in order that the cell temperature is held either equal to or slightly below the corresponding temperature in the control.

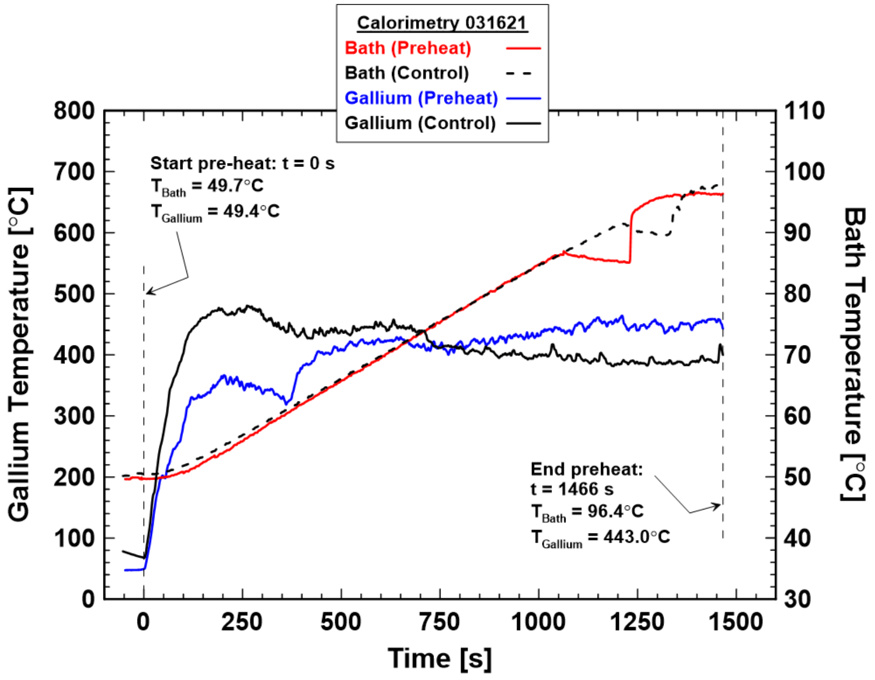

Figure 3. Cell and water bath temperature history in preheat and control

Temperatures and conditions during the preheat phase are summarized in Table 3. Parameters during the preheat are very similar to the control experiment, cf. Tables 2 and 3. Assuming the same 6.8 kg boil-off as in the control, the final mass of water in the bath at the end of the preheat phase is 190.6 kg.

Table 3. Power experiment preheat phase summary

Start t = 0	T_{Ga} = 49.4°C; T_{Bath} = 49.7°C
Water mass	197.4 kg
Supplies 1 and 2	~0.75 kA; ~21-25 V; ~17.3 kW
EMP	736 A; 1.35 V; 994 W
Glow discharge	Off
Gas flow	4000 sccm H2
WJ pump	Running for T_{Bath} < 90°C
End t = 1466 s	T_{Ga} = 443.0°C; T_{Bath} = 96.4°C
Water mass	190.6 kg (estimated)
Boil-off	6.8 kg (estimated)

Power phase

The electrode voltage (V), current (I) and power histories for both electrodes, corresponding to power supplies 1 and 2, are shown in Figs. 4 and 5. The power, VI, is calculated as the product of the voltage and current. Note that these data are plotted on a common time scale which is, however, independent of the scale used to plot cell and bath temperature in Fig. 3. Because the voltage and current are sampled at 5 kHz rather than 20 kHz as in the December, 2020 testing, the V, I and VI data for Supply 1 are plotted against an expanded time scale in Fig. 6. This figure indicates that 5 kHz sampling is sufficient to resolve the rapid current and voltage fluctuations. However, for accurate power and energy measurement, further reductions in sampling rate are not recommended. This is reinforced by the current data which is plotted in Fig. 6 using 1 kHz sampling. The deviations in indicated current compared to the 5 kHz sampling rate are significant. And, if the same sampling rate reduction were applied to the voltage as well, it is expected that the power, VI, would be impacted even further.

The start of the power phase is identified in the voltage and current data as the time that the current first begins to rise above the baseline level of about 0.75 kA used in the preheat phase. This happens at ~7.75 s for Supply 1 and slightly later at ~10.7 s for Supply 2. For Supply 1 the transition to the higher current (~1.5 kA) requires about 10 s, but only about 2 s for Supply 2. The end of the power phase corresponds to the time that the current drops to zero. This occurs at 69.64 s for Supply 1 and 69.46 s for Supply 2. From the power start and end times identified in Figs. 4 and 5 the power phase begins at 7.75 s and ends at 69.64 s, resulting in the power phase duration 69.64 - 7.75 = 61.89 s. The energy input to the cell from Supply 1 was calculated from the VI data using trapezoids as 2544 kJ and similarly 1464 kJ for Supply 2. Hence the total electrode energy input during the power phase was E_{Elect} = 4008 kJ.

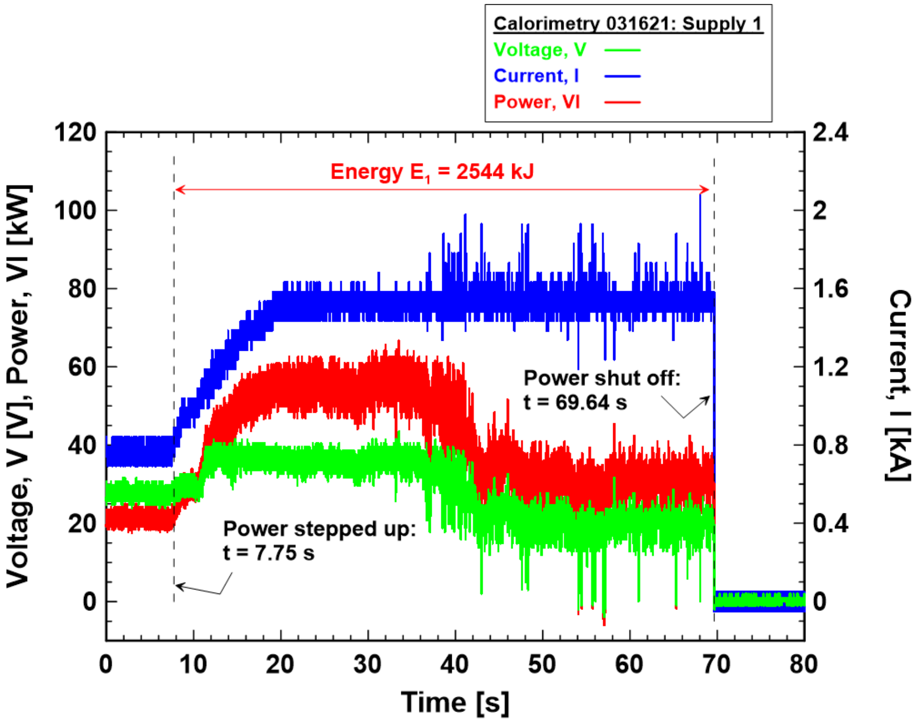

Figure 4. Electrode voltage, current and power during power phase for Supply 1

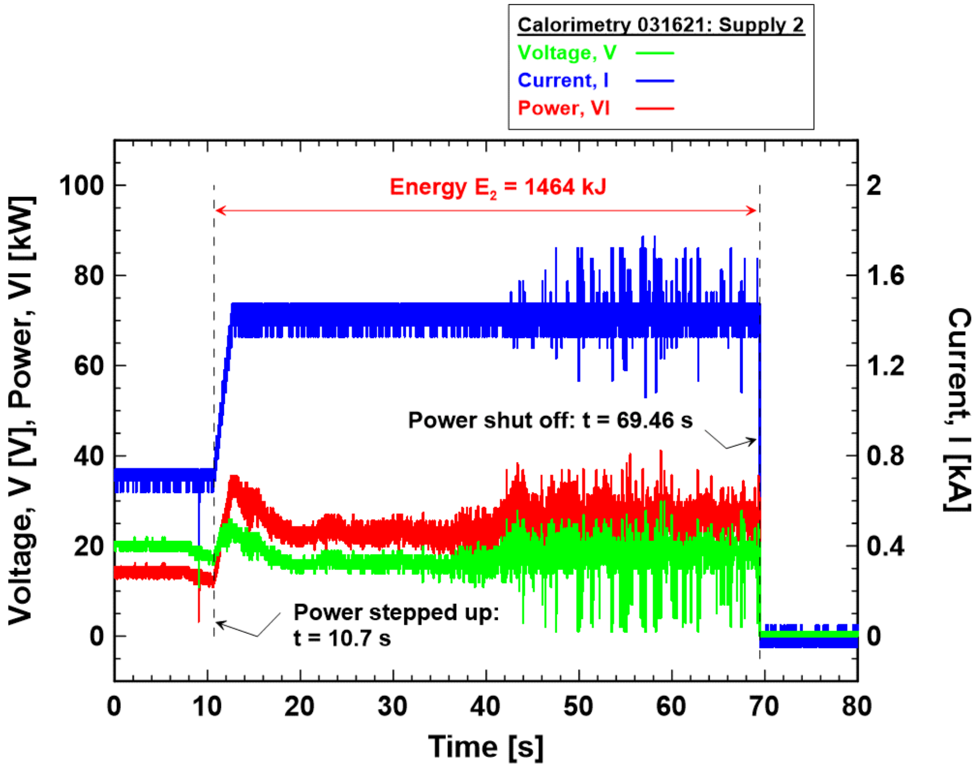

Figure 5. Electrode voltage, current and power during power phase for Supply 2

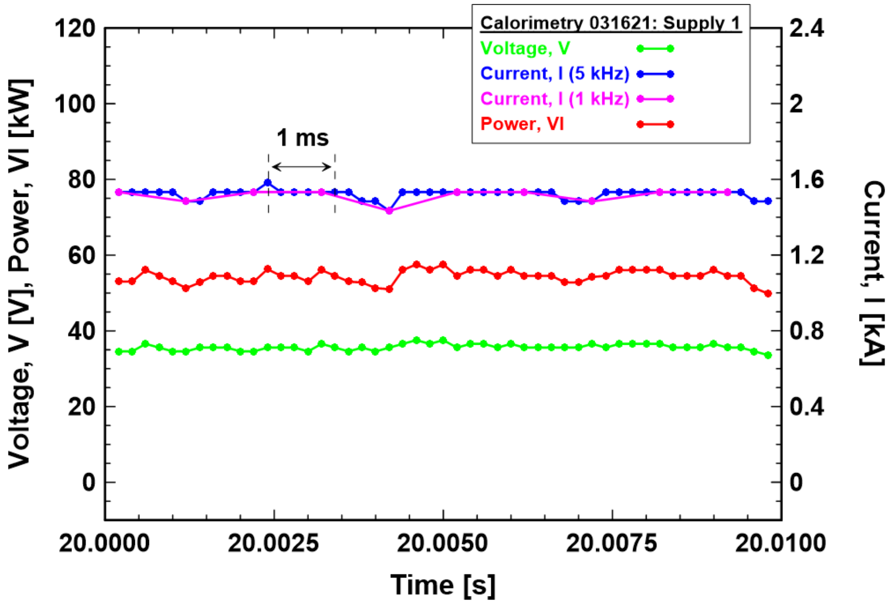

Figure 6. Electrode voltage, current and power for Supply 1 (expanded time scale)

The cell and bath temperatures during the power phase are plotted in Fig. 7. There is some difficulty in precisely identifying the power phase in this temperature plot because the DAS time stamps for the electrode power and temperature are independent. In Fig. 7 the start and end of the power phase are approximated as the beginning of the sharp gallium temperature rise at 1466 s and the beginning of the gallium temperature decay at 1519 s. These boundaries are not precise since the thermocouple probe in the cell is covered by a quartz sheath which increases its response time. The effect of the increased response time on the estimated duration of the power phase, 1519 - 1466 = 53 s, is expected to be reduced because similar and partially cancelling response delays are anticipated at both the start and end of the power phase. Still, the power phase duration calculated on the basis of cell temperature differs by 61.9 - 53 = 8.9 s from the actual power phase duration. This difference actually matters little in the calculation of plasma energy from the energy balance (1) since the energy contribution due to the bath temperature change, which is affected by the ambiguity in power phase duration, will be seen to be a small fraction of the net plasma energy. The temperatures and conditions present during the power phase are summarized in Table 4.

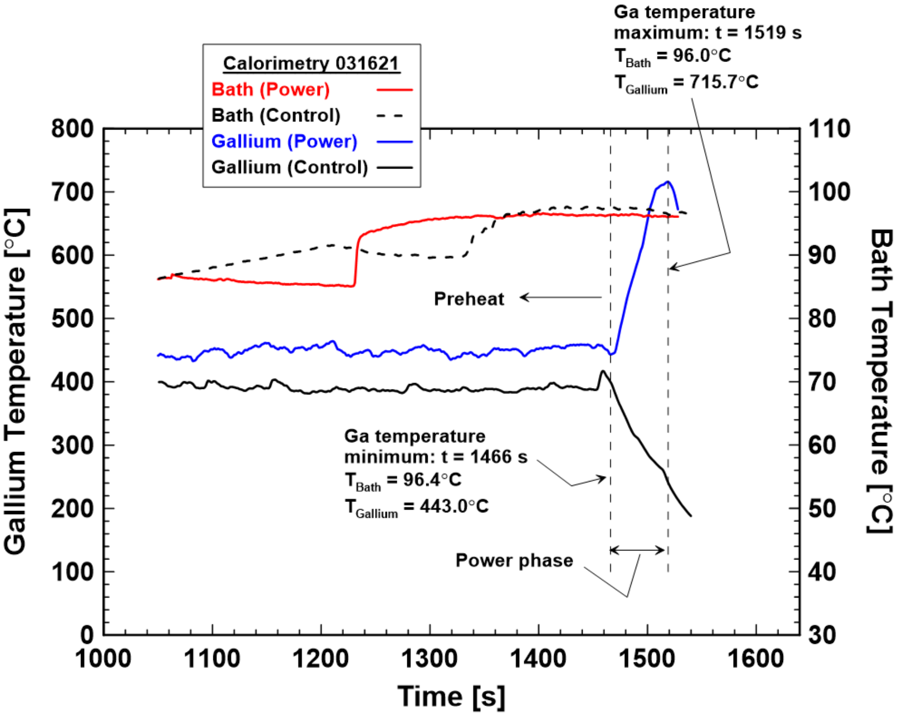

Figure 7. Cell and water bath temperature history in power phase

Table 4. Power phase summary

Start t = 1466 s	T_{Ga} = 443.0°C; T_{Bath} = 96.4°C
Water mass	190.6 kg (estimated)
Supply 1	E_1 = 2544 kJ
Supply 2	E_2 = 1464 kJ
Supply total	E_{Elect} = 4008 kJ
EMP	736 A; 1.35 V; 994 W
Glow discharge	0.53 A; 300 V; 159 W
Gas flow	4000 sccm H2 + 3 sccm O2
WJ pump	Off
End t = 1519 s	T_{Ga} = 715.7°C; T_{Bath} = 96.0°C
Water mass	184.1 kg
Boil-off	6.5 kg

Proper demarcation of the power phase

Note that the beginning of the power phase must coincide with start of the electrode current and power ramp-up to be consistent with the energy balance, Eq. (1). The term δm_w in (1) corresponds to the bath water boiled off following the end of the preheat phase since the control experiment accounts for water boiled off during the preheat only. And similarly E_{Elect} in (1) is the electrode energy added to the cell following the preheat. If the power phase start was taken as the time at which the current became stable at the stepped up level then the energy input during the ramp up would not be included in (1) but the water boil-off during the ramp period *would* be included in the δm_w term. Hence the inconsistency and corresponding error in calculation of the plasma energy release.

Plasma energy release

The bath water mass boiled off during the power phase was 6.5 kg and the bath water temperature change was -0.4°C since the water cooled slightly during this period. Hence the contributions to the plasma energy in (1) due to bath water enthalpy change and water vaporization are -321 and 14,742 kJ, respectively, as shown in Table 5. The contributions due to heat losses, EM pump input, thermal capacitance of the cell and related hardware, and input due to the glow discharge are 149, -62, -9, and -10 kJ, respectively. Summing these effects according to (1) results in the plasma energy release during the power phase:

$$E_{Plasma} = 10{,}481 \text{ kJ}$$

Note that the bath enthalpy change is responsible for only about 3% of this energy, so the uncertainty in identifying the power phase in the temperature plot has only a minor effect on the calculated plasma energy release. The gain is

$$\text{Gain} = \frac{E_{\text{Plasma}} + E_{\text{Elect}}}{E_{\text{Elect}}} = 3.615$$

That is, the plasma energy release is about 2.62 times the electrode energy input.

Table 5. Plasma energy release data

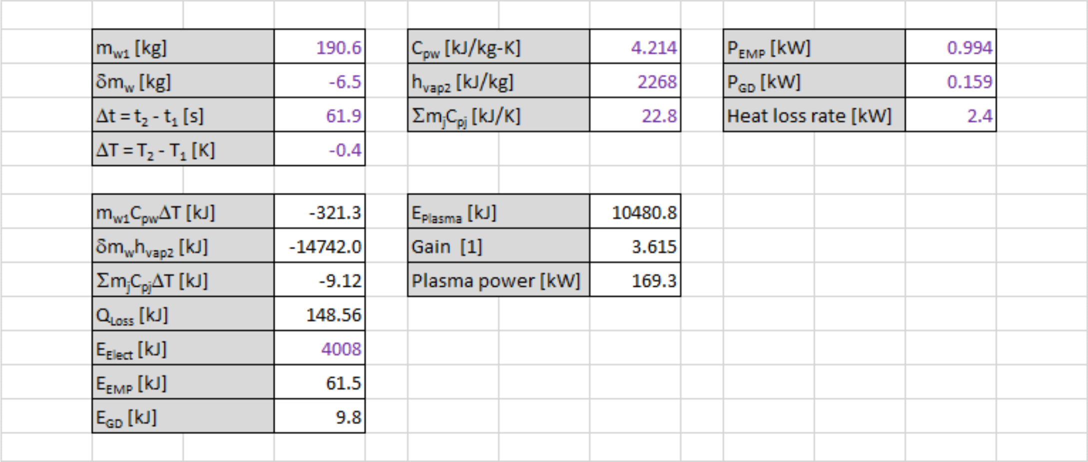

m_{w1} [kg]	190.6	C_{pw} [kJ/kg-K]	4.214	P_{EMP} [kW]	0.994
δm_w [kg]	-6.5	h_{vap2} [kJ/kg]	2268	P_{GD} [kW]	0.159
$\Delta t = t_2 - t_1$ [s]	61.9	$\Sigma m_j C_{pj}$ [kJ/K]	22.8	Heat loss rate [kW]	2.4
$\Delta T = T_2 - T_1$ [K]	-0.4				
$m_{w1} C_{pw} \Delta T$ [kJ]	-321.3	E_{Plasma} [kJ]	10480.8		
$\delta m_w h_{vap2}$ [kJ]	-14742.0	Gain [1]	3.615		
$\Sigma m_j C_{pj} \Delta T$ [kJ]	-9.12	Plasma power [kW]	169.3		
Q_{Loss} [kJ]	148.56				
E_{Elect} [kJ]	4008				
E_{EMP} [kJ]	61.5				
E_{GD} [kJ]	9.8				

The average plasma power release during the 61.9 s power phase is

$$P_{\text{Plasma}} = 169.3 \text{ kW}$$

However, the actual time distribution of plasma power release during the power phase is unknown. If most of the plasma energy is released during the later fraction of the power phase which excludes the power ramp-up period, then a better approximation of the plasma power is

$$P_{\text{Plasma}} = 210 \text{ kW (based on 50 s energy release period)}$$

If the electrode power remains at the average level of ~65 kW during the time that this increased plasma power release is occurring, then the local power gain is about 4.2. The implication that plasma power, at times during the power phase, considerably exceeds the average power is supported by the cell temperature data in Fig. 7. There it is seen that an inflection occurs in the data near 1495 s, resulting in a locally stronger rate of cell temperature rise.

Uncertainty in the estimate of plasma energy release is due primarily to uncertainty in the measurement of bath water boil-off. This uncertainty, about ±0.1 kg, results in only about ±2% uncertainty in plasma energy.